

Atom-atom entanglement characteristics in fiber-connected cavities system within the double-excitation space

YU XiangYang*, LI JianHong & LI XiaoBin

State Key Laboratory of Optoelectronic Materials and Technologies, Sun Yat-Sen University, Guangzhou 510275, China

Received February 6, 2012; accepted March 19, 2012; published online August 7, 2012

Starting from a rudimentary quantum-networks model that consists of two two-level confined atoms locating respectively in spatially-separated cavities coupled by fiber, we investigate the complex entanglement characteristics of the composite system analytically under the maximally initial entangled state that generates two excitations simultaneously during the temporal-evolution process. Our calculation clearly shows that, through mediating the atom-cavity coupling strength and photon-photon hopping rate appropriately, the entanglement dynamics displays some distinctive temporal properties differing from those obtained in one-excitation space, characterized partially by these newly quantum phenomena termed as entanglement sudden death and recurrence. Effectively, within the framework of two excitations, we suggest the purposeful manipulations of atomic entanglement communication for quantum networks.

quantum entanglement, cavity quantum electrodynamics, fiber-connected cavities

PACS number(s): 03.65.Ud, 03.67.Bg, 42.50.Dv

Citation: Yu X Y, Li J H, Li X B. Atom-atom entanglement characteristics in fiber-connected cavities system within the double-excitation space. *Sci China-Phys Mech Astron*, 2012, 55: 1813–1819, doi: 10.1007/s11433-012-4851-1

1 Introduction

Quantum entanglement, which essentially reveals the non-local correlation between localized subsystems without any classical analogue, has been generally recognized as the fundamental resource in efficiently implementing certain quantum information-related tasks [1]. By making use of such a notion, the most profound result associated with quantum entanglement should be the theoretical prediction and experimental demonstration of teleporting of an unknown coherent superposition state [2,3], which may offer us some conceivable physical models about quantum networks. Similar to conventional counterparts, a quantum network generally consists of local information processors responsible for coherent manipulation of quantum state, and

physical communication channels for transmitting information. Recently, a generic physical model capable of acting as the rudimentary quantum internet has been a focus of research for its potentiality in realizing scalable quantum computation. This physical model, namely, the atom-cavity-fiber-cavity-atom coupled system, is constructed by two two-level atoms trapped in fiber-coupled high-finesse cavities [4–7], and may offer us some pivotal advantages in practical applications. For instance, the atomic systems described by quantum electrodynamics are highly qualified to perform as qubits, as appropriate internal electronic states could coherently store information over a relatively long timescale. Based on this aforementioned physical model, highly reliable and robust quantum swap, controlled-Z and phase gates have been deterministically realized and reveal some potential perspectives for future quantum-information processing [8,9]. More recently, under different initial conditions (including $g_{a,b} \gg J$, $g_{a,b} \approx J$ and $g_{a,b} \ll J$),

*Corresponding author (email: cesyxy@mail.sysu.edu.cn)

researchers have discussed the detailed transfer behavior of quantum state between two two-level atoms in photonic-crystal coupled cavities within the context of a single excitation, which actually corresponds to the maximally initial entangled state $(|e_a\rangle|g_b\rangle+|e_b\rangle|g_a\rangle)/\sqrt{2}$ [10,11].

Liao et al. [12] also studied the efficient control of transporting a single photon in an array of coupled cavities by modulating the cavity frequency appropriately. On the basis of the previous study of quantum dynamics of a two-qubit composite system [13], in this work we extend the quantum physical model suggested by previous work [10,11], and consider another general and more complex case characterized by another type of maximally initial entangled state $(|e_a\rangle|e_b\rangle+|g_a\rangle|g_b\rangle)/\sqrt{2}$. It is evident that this type of entangled state could generate two excitations during the complex evolution process. Consequently, it can be anticipated that the outcomes obtained in two-excitation space will differ from those in previous studies [10,11], and thus may offer us some insights into the entanglement behavior in cavity quantum electrodynamics.

2 Theory

Figure 1(a) schematically depicts the physical configuration of the composite system under consideration, which consists of two two-level atoms confined in two spatially-separated and fiber-coupled optical cavities within a single mode. Under the resonant condition, which means that the atomic transition frequency is equal to the cavity oscillatory frequency, the associated Hamiltonian of the coupled quantum system in the interaction picture reads

$$H = i\hbar \sum_{i=a,b,j=1,2} [g_i (a_i^+ \sigma_i^- - \sigma_i^+ a_i)] + i\hbar J (a_1^+ a_2 - a_1 a_2^+), \quad (1)$$

where $\sigma_{a,b}^+$ and $\sigma_{a,b}^-$ are the atomic rising and lowering operators; $a_{1,2}^+$ and $a_{1,2}$ are the creating and annihilation operators of the single cavity-mode field, respectively. $g_{a,b}$ is the coupling strength of atomic dipole moment within the single cavity mode, which can be modulated by placing the atom in different positions in the cavity. J represents the photon hopping rate between the spatially-separated cavities, which is closely related to the distance between the cavities. The term $a_1^+ a_2$ ($a_1 a_2^+$) suggests that after a photon is annihilated in cavity 2 (1) and another photon will subsequently be generated in the cavity 1 (2). Here the photon can be treated as the good quantum-information carrier due to the low leakage out of an optical fiber and the capability of the photon to travel long distance with slight decoherence. Because we only consider the case of double excitations, the following concentrates on the entanglement dynamics of the maximally initial entangled state:

$$|\psi_0\rangle = (|e_a\rangle|e_b\rangle + |g_a\rangle|g_b\rangle)/\sqrt{2}. \quad (2)$$

Therefore we need to construct the following nine standard product states to describe the total evolution of the coupled quantum system, expressed as:

$$|9\rangle = |g_a\rangle|g_b\rangle|0\rangle_1|0\rangle_2, \quad (3a)$$

$$|8\rangle = |e_a\rangle|e_b\rangle|0\rangle_1|0\rangle_2, \quad (3b)$$

$$|7\rangle = |g_a\rangle|e_b\rangle|1\rangle_1|0\rangle_2, \quad (3c)$$

$$|6\rangle = |e_a\rangle|g_b\rangle|0\rangle_1|1\rangle_2, \quad (3d)$$

$$|5\rangle = |g_a\rangle|g_b\rangle|1\rangle_1|1\rangle_2, \quad (3e)$$

$$|4\rangle = |g_a\rangle|e_b\rangle|0\rangle_1|1\rangle_2, \quad (3f)$$

$$|3\rangle = |e_a\rangle|g_b\rangle|1\rangle_1|0\rangle_2, \quad (3g)$$

$$|2\rangle = |g_a\rangle|g_b\rangle|2\rangle_1|0\rangle_2, \quad (3h)$$

$$|1\rangle = |g_a\rangle|g_b\rangle|0\rangle_1|2\rangle_2. \quad (3i)$$

It can be seen that the temporal evolution of the null-excitation quantum state $|9\rangle$ remains invariant under the action of the Hamiltonian. Thus, we could ignore its effects on the entanglement dynamics and simplify our calculation. Figure 1(b) explicitly illustrates the allowed atomic dipole-moment transition and photon exchange between the associated quantum states. Therefore the entanglement behavior within the double-excitation space under consideration involves eight eigenvalues. Furthermore, it should be noted that some new quantum states such as $|4\rangle$, $|3\rangle$, $|2\rangle$ and $|1\rangle$ emerge because of the photon interchange between the cavities through the optical fiber, which is not possible for the case of two isolated cavities without any connection.

According to the Schrödinger equation

$$i\hbar \frac{\partial |\psi(t)\rangle}{\partial t} = H |\psi(t)\rangle, \quad (4)$$

in which $|\psi(t)\rangle = \sum_{k=1}^8 C_k(t) |k\rangle$ is called the total wave function, the first-order coupled ordinary differential equations describing the composite system dynamics are obtained, given by

$$\dot{C}_8(t) = -g_a C_7(t) - g_b C_6(t), \quad (5a)$$

$$\dot{C}_7(t) = g_a C_8(t) - g_b C_5(t) + J C_4(t), \quad (5b)$$

$$\dot{C}_6(t) = g_b C_8(t) - g_a C_5(t) - J C_3(t), \quad (5c)$$

$$\dot{C}_5(t) = g_b C_7(t) + g_a C_6(t) - \sqrt{2} J C_2(t) + \sqrt{2} J C_1(t), \quad (5d)$$

$$\dot{C}_4(t) = -g_b C_1(t) - J C_7(t), \quad (5e)$$

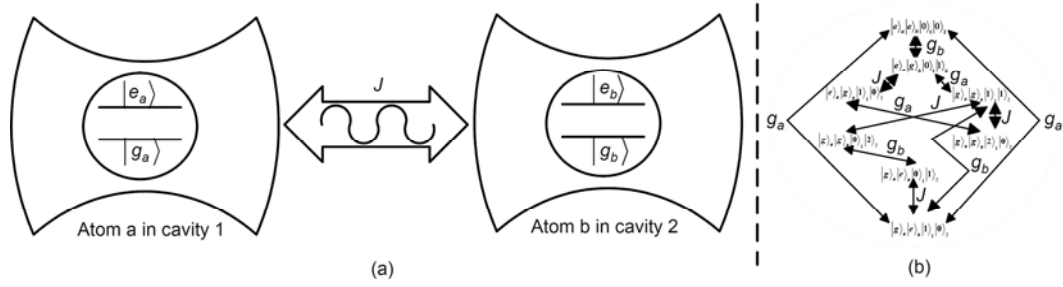


Figure 1 (a) Schematic representation of the composite system under consideration. The two two-level atoms are respectively embedded in local cavities coupled by an optical fiber, which performs the photon exchange between the spatially-separated cavities within hopping rate J . (b) Illustrates the allowed atomic dipole-moment transition and photon hopping between the corresponding quantum states.

$$\dot{C}_3(t) = -g_a C_2(t) + J C_6(t), \quad (5f)$$

$$\dot{C}_2(t) = g_a C_3(t) + \sqrt{2} J C_5(t), \quad (5g)$$

$$\dot{C}_1(t) = g_b C_4(t) - \sqrt{2} J C_5(t). \quad (5h)$$

By employing the Laplace transform theory and the coupled initial condition of the system ($|e_a\rangle|e_b\rangle + |g_a\rangle|g_b\rangle$) $|0\rangle_1|0\rangle_2 / \sqrt{2}$, we derived the analytical solutions as thus

$$C_8(t) = \frac{\sqrt{2}}{4} \sum_{j=1}^8 A_1^{-1} \left\{ \begin{aligned} & (f_{ab}^2 + 2J^4 - 2\sqrt{2}J^4) g_{ab}^2 + (g_{ab}^4 - 4\sqrt{2}f_{ab}^2) J^2 + 4J^6 + K_j^6 \\ & + [(1 + 4J^2 - 2\sqrt{2}J^2) g_{ab}^2 + 3f_{ba}^2 + 9J^4] K_j^2 + (6J^2 + 2g_{ab}^2) K_j^4 \end{aligned} \right\} e^{K_j t}, \quad (6a)$$

$$C_7(t) = \frac{g_a}{\sqrt{2}} \sum_{j=1}^8 A_2^{-1} \left\{ \begin{aligned} & [f_{ab}^2 + g_{ba}^4 + (-2\sqrt{2}g_{ba}^2 + 2g_{ab}^2 + g_b^2) J^2 + 4J^4] K_j^2 \\ & + g_b^2 (g_a^2 - \sqrt{2}J^2) g_{ab}^2 + (5J^2 + 2g_a^2) K_j^4 + K_j^6 \end{aligned} \right\} e^{K_j t}, \quad (6b)$$

$$C_6(t) = \frac{g_b}{\sqrt{2}} \sum_{j=1}^8 A_2^{-1} \left\{ \begin{aligned} & [f_{ab}^2 - g_{ba}^4 + (2\sqrt{2}g_{ab}^2 + 2g_{ab}^2 + g_a^2) J^2 + 4J^4] K_j^2 \\ & + g_a^2 (g_b^2 + \sqrt{2}J^2) g_{ab}^2 + (5J^2 + 2g_b^2) K_j^4 + K_j^6 \end{aligned} \right\} e^{K_j t}, \quad (6c)$$

$$C_5(t) = \frac{-g_a g_b}{\sqrt{2}} \sum_{j=1}^8 A_3^{-1} \left\{ \begin{aligned} & -2f_{ab}^2 + (\sqrt{2} - 1) g_{ab}^2 J^2 + 2\sqrt{2}J^4 \\ & + 2[(\sqrt{2}J^2 - 1) J^2 - g_{ab}^2] K_j^2 - 2K_j^4 \end{aligned} \right\} e^{K_j t}, \quad (6d)$$

$$C_4(t) = \frac{-g_a J}{\sqrt{2}} \sum_{j=1}^8 A_3^{-1} \left\{ \begin{aligned} & -(2\sqrt{2} + 1) f_{ab}^2 + 2(g_{ab}^2 - \sqrt{2}g_a^2) J^2 + 4J^4 \\ & + [5J^2 + 2g_a^2 - (2\sqrt{2} + 1) g_b^2] K_j^2 + K_j^4 + g_a^4 \end{aligned} \right\} e^{K_j t}, \quad (6e)$$

$$C_3(t) = \frac{g_b J}{\sqrt{2}} \sum_{j=1}^8 A_3^{-1} \left\{ \begin{aligned} & -(2\sqrt{2} + 1) f_{ab}^2 + 2(g_{ab}^2 - \sqrt{2}g_b^2) J^2 + 4J^4 \\ & + [5J^2 + 2g_b^2 - (2\sqrt{2} + 1) g_a^2] K_j^2 + K_j^4 + g_b^4 \end{aligned} \right\} e^{K_j t}, \quad (6f)$$

$$C_2(t) = \frac{f_{ab} J}{\sqrt{2}} \sum_{j=1}^8 A_4^{-1} \left\{ \begin{aligned} & [2(\sqrt{2} + 1) g_b^2 - g_a^2 + (2\sqrt{2} + 1) J^2] K_j^2 \\ & + g_b^4 - f_{ab}^2 + \sqrt{2}g_{ba}^2 J^2 + (2\sqrt{2} + 1) K_j^4 \end{aligned} \right\} e^{K_j t}, \quad (6g)$$

$$C_1(t) = \frac{-f_{ab} J}{\sqrt{2}} \sum_{j=1}^8 A_4^{-1} \left\{ \begin{aligned} & [2(\sqrt{2} + 1) g_a^2 - g_b^2 + (2\sqrt{2} + 1) J^2] K_j^2 \\ & + g_a^4 - f_{ab}^2 - \sqrt{2}g_{ba}^2 J^2 + (2\sqrt{2} + 1) K_j^4 \end{aligned} \right\} e^{K_j t}, \quad (6h)$$

where $g_{ab}^m = g_a^m + g_b^m$, $g_{ba}^m = g_a^m - g_b^m$ ($m = 2, 4, 6$), $f_{ab}^2 = g_a^2 g_b^2$,

$$A_1 = \left\{ \begin{aligned} & (f_{ab}^2 + 6J^4 - 2\sqrt{2}J^4) g_{ab}^2 + (3 - 2\sqrt{2}) J^2 g_{ab}^4 + g_{ab}^6 + 6f_{ab}^2 J^2 + 4J^6 \\ & + [(18 - 4\sqrt{2}) J^2 g_{ab}^2 + 6g_{ab}^4 + 6f_{ab}^2 + 18J^4] K_j^2 + (18J^2 + 9g_{ab}^2) K_j^4 + 4K_j^6 \end{aligned} \right\}, \quad (7a)$$

$$A_2 = \left\{ \begin{aligned} &2 \left[\left(g_{ab}^4 + f_{ab}^2 + \left(6 + (3 - 2\sqrt{2}) g_{ab}^2 \right) J^2 + (6 - 2\sqrt{2}) J^4 \right) g_{ab}^2 + 4J^6 \right] K_j \\ &+ \left[12g_{ab}^4 + \left(12 + (36 - 8\sqrt{2}) J^2 \right) g_{ab}^2 + 36J^4 \right] K_j^3 + \left(18g_{ab}^2 + 36J^2 \right) K_j^5 + 8K_j^7 \end{aligned} \right\}, \tag{7b}$$

$$A_3 = \left\{ \begin{aligned} &2 \left(6J^2 + g_{ab}^2 \right) f_{ab}^2 + 2g_{ab}^6 + \left[4(3 - \sqrt{2}) J^2 + (6 - 4\sqrt{2}) g_{ab}^2 \right] g_{ab}^2 J^2 + 8J^6 \\ &+ \left[12f_{ab}^2 + 12g_{ab}^4 + (36 - 8\sqrt{2}) g_{ab}^2 J^2 + 36J^4 \right] K_j^2 + \left(36J^2 + 18g_{ab}^2 \right) K_j^4 + 8K_j^6 \end{aligned} \right\}, \tag{7c}$$

$$A_4 = \left\{ \begin{aligned} &2 \left(6J^2 + g_{ab}^2 \right) f_{ab}^2 + 2g_{ab}^6 + \left(4(3 - \sqrt{2}) J^2 + (6 - 4\sqrt{2}) g_{ab}^2 \right) g_{ab}^2 J^2 + 8J^6 \left] K_j \right. \\ &+ \left. \left[12f_{ab}^2 + 12g_{ab}^4 + (36 - 8\sqrt{2}) J^2 g_{ab}^2 + 36J^4 \right] K_j^3 + \left(36J^2 + 18g_{ab}^2 \right) K_j^5 + 8K_j^7 \right\}. \tag{7d}$$

K_j is one of the roots of the following characteristic equation

$$f_{ab}^2 g_{ba}^4 + \left\{ f_{ab}^2 + g_{ab}^6 + \left[(3 - 2\sqrt{2}) g_{ab}^4 + 6f_{ab}^2 + (6 - 2\sqrt{2}) J^2 \right] g_{ab}^2 J^2 + 4J^6 \right\} K^2 + \left\{ 12J^4 + \left[(9 - 2\sqrt{2}) g_{ab}^2 + 3g_{ab}^4 + 3f_{ab}^2 \right] J^2 \right\} K^4 + 3(2J^2 + g_{ab}^2) K^6 + K^8 = 0. \tag{8}$$

One should note that from eqs. (6e) to (6h), the emergence of new quantum states is entirely determined by the parameter J , consistent with our preceding intuition.

To quantify and trace the amount of entanglement appropriately, Wootters concurrence [14] is employed, defined mathematically as:

$$\hat{C}_{ab}(t) = 2 \max \left\{ 0, \sqrt{\lambda_1} - \sqrt{\lambda_2} - \sqrt{\lambda_3} - \sqrt{\lambda_4} \right\}, \tag{9}$$

where $\lambda_{i=1,2,3,4}$, arranged in a decreasing order, as are the eigenvalues of the density matrix operator $\rho_{ab} \tilde{\rho}_{ab}$, where $\tilde{\rho}_{ab} = \sigma_y \otimes \sigma_y \rho_{ab}^* \sigma_y \otimes \sigma_y$ with σ_y being Pauli matrix and ρ_{ab}^* denoting the complex conjugation of ρ_{ab} . Concurrence varies from 1 for a maximally entangled state to 0 for

a completely separable state. By exploiting the physical insight of concurrence, the qualitatively new phenomena, namely entanglement sudden death (ESD) and recurrence (ESR), have been investigated extensively under the regimes of Markovian and non-Markovian approximations [15,16], respectively. Generally speaking, we could apply concurrence to quantify the entanglement amount of various subsystems such as atom-atom subsystem, atom-cavity subsystem and cavity-cavity subsystems. The fundamental interest of this paper is to focus on the atom-atom entanglement dynamics for its potential applications in future quantum network. Consequently, by taking the partial trace over the cavity-cavity subsystem, the reduced time-dependent density matrix for the atomic system in terms of the basis states $|e_a\rangle|e_b\rangle$, $|e_a\rangle|g_b\rangle$, $|g_a\rangle|e_b\rangle$ and $|g_a\rangle|g_b\rangle$ can be written as:

$$\rho_{ab}(t) = \begin{pmatrix} |C_8|^2 & 0 & 0 & C_8 C_9^* \\ 0 & |C_7|^2 + |C_4|^2 & C_4 C_6^* + C_7 C_3^* & 0 \\ 0 & C_4^* C_6 + C_7^* C_3 & |C_6|^2 + |C_3|^2 & 0 \\ C_8^* C_9 & 0 & 0 & |C_9|^2 + |C_5|^2 + |C_2|^2 + |C_1|^2 \end{pmatrix}. \tag{10}$$

Thus the mathematical expression for concurrence should take the exact form

$$\hat{C}_{ab}(t) = 2 \max \left\{ \begin{aligned} &0, |C_8| |C_9| - \left[\left(|C_7|^2 + |C_4|^2 \right) \left(|C_6|^2 + |C_3|^2 \right) \right]^{1/2}, \\ &\left[\left(C_4 C_6^* + C_7 C_3^* \right) \left(C_4^* C_6 + C_7^* C_3 \right) \right]^{1/2} - |C_8| \left(|C_9|^2 + |C_5|^2 + |C_2|^2 + |C_1|^2 \right)^{1/2} \end{aligned} \right\}. \tag{11}$$

According to the explicit definition of concurrence, we continue to calculate the temporal evolution of atom-atom entanglement under three different initial circumstances. In first case, the coupling strength of atom-cavity is much larger than that of the photon-photon hopping strength, which can be expressed as $g_{a,b} \gg J$. The second case is that $g_{a,b}$ and J is comparable in magnitude; that is, $g_{a,b} \approx J$.

For the third case, it corresponds to the condition $g_{a,b} \ll J$.

3 Results and discussion

As schematically depicted in Figures 2 and 3, which respec-

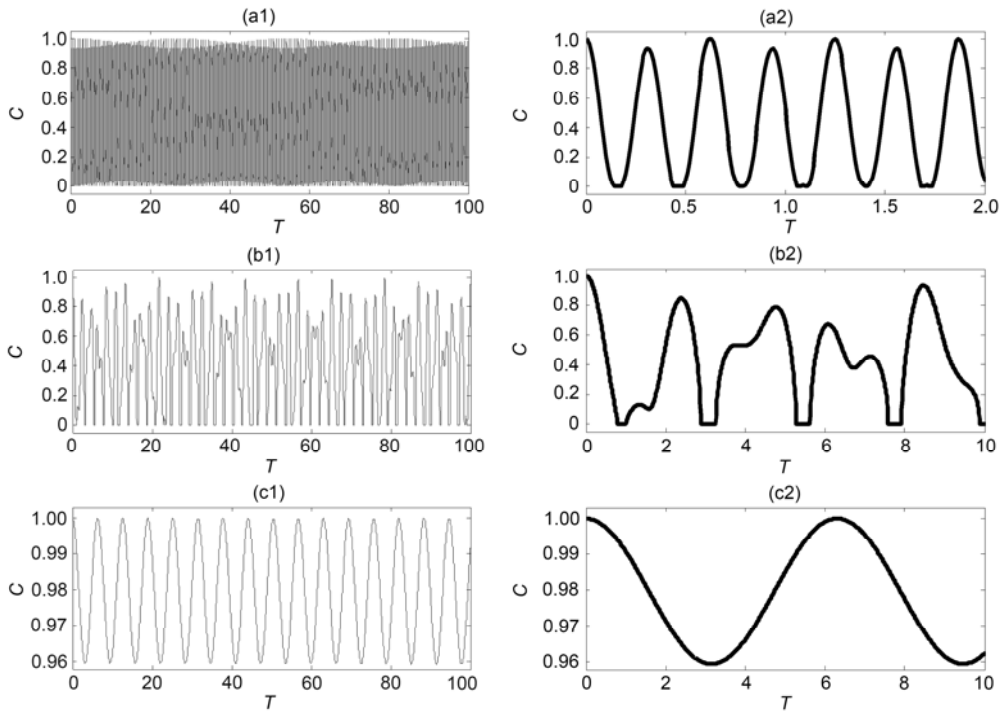


Figure 2 Concurrence evolution as a function of time for $J=1$ and (a) ((a1) and (a2)) $g_a=10, g_b=10$; (b) ((b1) and (b2)) $g_a=1.5, g_b=1.5$; (c) ((c1) and (c2)) $g_a=0.1, g_b=0.1$. The right graphics are the zoomed views of those on the left.

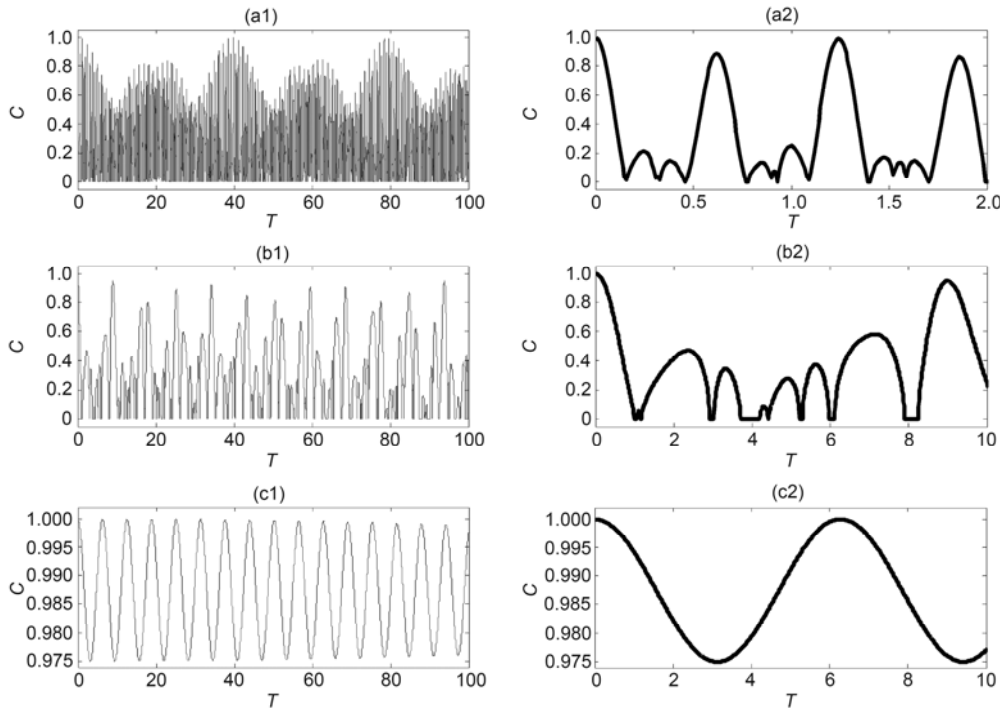


Figure 3 Concurrence evolution as a function of time for $J=1$ and (a) ((a1) and (a2)) $g_a=10, g_b=5$; (b) ((b1) and (b2)) $g_a=1.5, g_b=0.75$; (c) ((c1) and (c2)) $g_a=0.1, g_b=0.05$. The right graphics are the zoomed views of those on the left.

tively correspond to the equal ($g_a = g_b$) and unequal ($g_a \neq g_b$) atom-cavity coupling strength, the entanglement dynamics of atom-atom subsystem are quite distinctive un-

der differing initial conditions. In the $g_{a,b} \gg J$ and $g_a = g_b$ case, where the atom-cavity coupling strength dominates the whole evolution process and is involved in shaping entan-

lement, the temporal evolution of atom-atom entanglement displays approximately quasi-periodic oscillation in magnitude with rapid frequency, which is directly proportional to these parameters g_a and g_b . In contrast to the corresponding results in refs. [11,12], the fundamental feature that a fast-oscillation pattern is superposed with a slowly varying oscillatory envelope has disappeared here. Mathematically, this trait originates from different timescales $g_{a,b}$ and J dominates. It can be seen that $g_{a,b} \gg J$, $g_{a,b}$ is responsible for the rapid oscillation curve and J for the slowly varying envelop. Here the phenomenon can be attributed to different initial entangled states. For the maximally initial entangled state $(|e_a\rangle|e_b\rangle + |g_a\rangle|g_b\rangle)/\sqrt{2}$ under consideration here, two excitations appear during the evolution process, while only one excitation emerges for another maximally initial entangled state $(|e_a\rangle|g_b\rangle + |g_a\rangle|e_b\rangle)/\sqrt{2}$ [11,12]. The bidirectional and simultaneous communication of two photons generated in the two-excitation space could reduce the timescale effected by J , when it is compared to the timescale in one-way transmission of a single photon through the optical fiber. The reduced timescale caused by the influence of J thus makes the slowly varying envelope not obvious within the two-excitation space. The simultaneousness mentioned hereby refers to the input of the photon into the communication channel and the corresponding output that occurs precisely at the same time, which can be satisfied by assuming $g_a = g_b$. Thus each atom's time-evolution is symmetrical and identical. Naturally one can anticipate that when the composite system loses the simultaneousness (by setting $g_a \neq g_b$), the slowly varying envelope becomes remarkable, as clearly demonstrated in Figure 3(b). In addition, under this limit of large coupling strength, it can be observed that the atom-atom coupled system suffers from ESD and ESR due to the remarkable atomic dipole-moment transition induced by strong atom-cavity coupling strength. ESD and ESR appear alternatively as a function of time and indicate the dramatic exchange of entanglement resource between atom-atom subsystem and other coupled subsystems.

However, ESD and ESR disappear completely when it comes to the regime that $g_{a,b} \ll J$ (refer to Figures 2(c) and 3(c)). It can be shown that the entanglement behavior undergoes a cosine oscillation via time, whose amplitude quantified by concurrence ranges approximately from 0.92 to 1. This feature reflects the slight repetitive communication of entanglement between atom-atom subsystem and other subsystems. That is because, due to the weak coupling strength and the two-way propagation of photons within the two-excitation space, most entanglement resource could be preserved in the atomic system. Moreover, when the value of J becomes relatively higher, the spatial distance between the cavities can be considered negligible. Therefore, within

the two-excitation space, the distinctive property of entanglement from extremely different coupling strengths provides us with some useful clues to manipulate quantum systems efficiently.

We now turn to another case in which g_a and g_b are comparable to J in magnitude. Unlike the two extreme situations mentioned above, the atom-atom entanglement dynamics with irregular oscillation frequency seems to be chaotic and unpredictable. The complex process actually results from the violent competition between various subsystems which intrinsically contend for the entanglement resource. Under this condition such that $g_{a,b} \approx J$, no individual evolution of the quantum state predominates over the whole process. On the contrary, all quantum states interplay and depend strongly on each other as time processes. Here one unique feature that characterizes the complete loss of atom-atom entanglement with relatively long time emerges, as opposed to the quasi-cosine oscillation of atomic entanglement for the other two cases ($g_{a,b} \gg J$ and $g_{a,b} \ll J$, respectively). This trait also reflects the mechanism of competition for the entanglement resource between different subsystems. Consequently, the aforementioned characteristics within the framework of two excitations reveal some essential properties of atom-atom entanglement behavior in cavity quantum electrodynamics.

Finally, we come to discuss briefly the experimental feasibility of the double-excitation physical architecture within the framework of current technologies. In recent years, the successful engineering of quantum systems on single-atom single-photon level in high-finesse cavities and the realization of perfect fiber-cavity coupling with efficiency larger than 99.97% can convincingly guarantee the practicability of this physical model [17–19]. Furthermore, a high-finesse cavity can protect photons from dissipation caused by ambient environment for a relatively longer time scale.

4 Conclusion

Thus, we have investigated the atom-atom entanglement behavior analytically and numerically within the two-excitation space. The physical architecture under consideration is constructed by two two-level atoms trapped respectively in two spatially-separated and fiber-coupled cavities. Under three different initial conditions (including $g_{a,b} \gg J$, $g_{a,b} \approx J$ and $g_{a,b} \ll J$), the entanglement characteristics within the two-excitation space prove to be quite different from those obtained in the single-excitation space. By setting the ratio of $g_{a,b}$ to J appropriately, we can accomplish the efficient manipulation of atom-atom entanglement behaviors like accelerating or suppressing the emergence of ESD and ESR. Our analysis may offer some useful guidelines for distributing and preserving entanglement in complex quantum networks.

This work was supported by the National Basic Research Program of China (Grant No. 2012CB921900), the National Natural Science Foundation of China (Grant No. 10574166) and the Guangdong Natural Science Foundation (Grant No. 8151027501000062).

- 1 Horodecki R, Horodecki P, Horodecki M, et al. Quantum entanglement. *Rev Mod Phys*, 2009, 81: 865–942
- 2 Bennett C H, Brassard G, Crepeau C, et al. Teleporting an unknown quantum state via dual classical and Einstein-Podolsky-Rosen channels. *Phys Rev Lett*, 1993, 70: 1895–1899
- 3 Bouwmeester D, Pan J W, Mattle K, et al. Experimental quantum teleportation. *Nature*, 1997, 390: 575–579
- 4 Cirac J I, Zoller P, Kimble H J, et al. Quantum state transfer and entanglement distribution among distant nodes in a quantum network. *Phys Rev Lett*, 1997, 78: 3221–3224
- 5 Serafini A, Mancini S, Bose S. Distributed quantum computation via optical fibers. *Phys Rev Lett*, 2006, 96: 010503
- 6 Kimble H J. The quantum internet. *Nature*, 2008, 453: 1023–1030
- 7 Duan L M, Monroe C. Quantum networks with trapped ions. *Rev Mod Phys*, 2010, 82: 1209–1224
- 8 Yin Z Q, Li F L. Multiatom and resonant interaction scheme for quantum state transfer and logical gates between two remote cavities via an optical fiber. *Phys Rev A*, 2007, 75: 012324
- 9 Yang Z B, Wu H Z, Su W J, et al. Quantum phase gates for two atoms trapped in separate cavities within the null- and single-excitation subspaces. *Phys Rev A*, 2009, 80: 012305
- 10 Zhang K, Li Z Y. Transfer behavior of quantum states between atoms in photonic crystal coupled cavities. *Phys Rev A*, 2010, 81: 033843
- 11 Yang W L, Yin Z Q, Xu Z Y, et al. Quantum dynamics and quantum state transfer between separated nitrogen-vacancy centers embedded in photonic crystal cavities. *Phys Rev A*, 2011, 84: 043849
- 12 Liao J Q, Gong Z R, Zhou L, et al. Controlling the transport of single by tuning the frequency of either one or two cavities in an array of coupled cavities. *Phys Rev A*, 2010, 81: 042304
- 13 Yu X Y, Li J H, Li X B. Non-zero quantum discord at finite temperature. *Sci China-Phys Mech Astron*, 2012, 55: 815–821
- 14 Wootters W K. Entanglement of formation of an arbitrary state of two qubits. *Phys Rev Lett*, 1998, 80: 2245–2248
- 15 Yu T, Eberly J H. Sudden death of entanglement. *Science*, 2009, 323: 598–601
- 16 Bellomo B, Franco R L, Compagno G. Non-Markovian effects on the dynamics of entanglement. *Phys Rev Lett*, 2007, 99: 160502
- 17 Wilk T, Webster S C, Kuhn A, et al. Single-atom single-photon quantum interface. *Science*, 2007, 317: 488–490
- 18 Hijlkema M, Weber B, Specht H P, et al. A single-photon server with just one atom. *Nat Phys*, 2007, 3: 253–255
- 19 Spillane S M, Kippenberg T J, Painter O J, et al. Ideality in a fiber-taper-coupled microresonator system for application to cavity quantum electrodynamics. *Phys Rev Lett*, 2003, 91: 043902